Some Aspects of Nitrogen Addition and Removal During Special Melting and Processing of Iron and Nickel Base-Alloys

E.C. Young and A. Mitchell

University of British Columbia
Department of Metals and Materials Engineering
6350 Stores Road, Vancouver, BC V6T 1Z4

(Received August 14, 2000; final form September 18, 2000)

ABSTRACT

In this work we review the published information on the exchange of nitrogen across the gas/metal interface in the case of liquid iron- and nickel-base alloys. Although the thermochemistry of these systems is reasonably well-established, it is clear that the kinetics of the reactions involved are rather complex and hence not as well defined. The role of precipitated nitrides is also considered, since this feature is an integral part of the use of filters as well as being a core facet of the nitride removal reaction in several of the processes surveyed. We also review the present position in respect of the production of high-nitrogen alloys, including the role of systems relying on the presence of N^+ ions to establish concentrations greater than those predicted by Sieverts' Law. We conclude that the basic information needed to establish a rational production route for any given alloy affected by nitrogen content is available, but that a very careful consideration of all the factors involved is required before defining such a route.

INTRODUCTION

The inevitability of reaction between liquid metals and the atmosphere has long been recognized, and control of this reaction is a key point in alloy production. In general, high-quality alloys are "clean" alloys, i.e. have low inclusion content; particularly in the case of oxide contamination, but limits for nitrogen content although not as universally defined, are also critical to overall mechanical behaviour. In some steels, the effect of nitrogen on properties is desirable, as it can impart strength, increase hardenability, assist grain refinement and act as an austenite stabilizer. In other alloys, nitrogen may be regarded as a harmful impurity that is often stabilized by the addition of strong nitride formers such as titanium, resulting in precipitation of nitrides and/or carbonitrides, the presence of which may or may not be beneficial to the desired microstructure. In the case of nickel-base superalloys, the precipitation of titanium nitrides is highly undesirable, since the precipitates control fatigue and fracture behaviour, and also modify the carbide precipitation in carbon-containing alloys. Additionally, the incidence of microporosity, particularly in equiax-cast superalloys, has been found to increase rapidly with an increase in nitrogen content /1/. The stringent specifications for superalloys in aerospace applications are directed towards the elimination of these types of defects.

Clearly, control of nitrogen to an optimum level is an important factor for product quality, and to this end, a considerable body of work is documented in the literature, studying both the thermodynamic and kinetic factors involved in predicting the nitrogen levels of particular alloys under specific processing conditions. This paper reviews the fundamentals of these processes, with a particular emphasis on the subtleties that arise for the case of special processing routes such as vacuum induction melting (VIM), vacuum arc remelting (VAR), electroslag remelting (ESR), arc-slag melting (ASM),

electron beam melting (EBM) and plasma arc remelting (PAR).

NITROGEN SOLUBILITY

As with all molecular gases, it is found that diatomic nitrogen gas invariably dissolves in liquid metals as atoms, in a reaction involving transport processes within one or both of the bulk phases, as well as the interfacial chemical step or phase boundary reaction. The overall reaction can be written as

$$N_2\,(g) = 2[N]\ \text{(in liquid metal)} \qquad (1)$$

and is at equilibrium when the partial molar free energy of nitrogen in the metallic solution is equal to the molar free energy of nitrogen in the gaseous phase /2/. This equilibrium can be written

$$K = \frac{a_N}{(p_{N_2})^{1/2}} \qquad (2)$$

where K is the equilibrium constant, p_{N2} is the partial pressure of nitrogen above the bath and a_N is the chemical activity of nitrogen in the bath. Generally, the infinitely dilute solution of nitrogen in the pure metal is taken as the reference state such that

$$\lim_{\%N \to 0} \frac{a_n}{\%N} = f_n = 1 \qquad (3)$$

where f_n is the Henrian activity coefficient. If it is assumed that nitrogen obeys Henry's law (a_n = [wt % N]f_n), then the concentration of nitrogen in the metal is given by Sieverts' law

$$[wt\%N] = k(T)p_{N_2}^{1/2} \qquad (4)$$

where k(T) is the temperature dependent Sieverts' constant, evaluated at equilibrium concentration at temperature T with gaseous N_2 at 1 atm pressure. In higher order alloys, the standard reference state is still referred to, but depending on the interaction coefficient between nitrogen and the additional elements, f_n will have a value that is greater or less than unity. The activity coefficient of nitrogen in the alloy is determined by

$$f_n = \left[\frac{\%N(puremetal)}{\%N(alloy)}\right]_{P_{N2},T} \qquad (5)$$

While the solubility of nitrogen in iron alloys had been measured by several researchers before 1960, it appears that the definitive study was made by Pehlke and Elliott /3/, who measured the solubility in pure iron as a function of temperature and pressure using the Sieverts' method. They determined the nitrogen solubility at 1600°C to be 0.0451 wt % N at 1 atm nitrogen pressure, a value that has been reproduced several times and as recently as 1985 by Rao and Lee /4/. It was determined that Sieverts' Law is obeyed at nitrogen pressures up to 1 atm, as can be seen in Figure 1, and the temperature coefficient of the solubility is

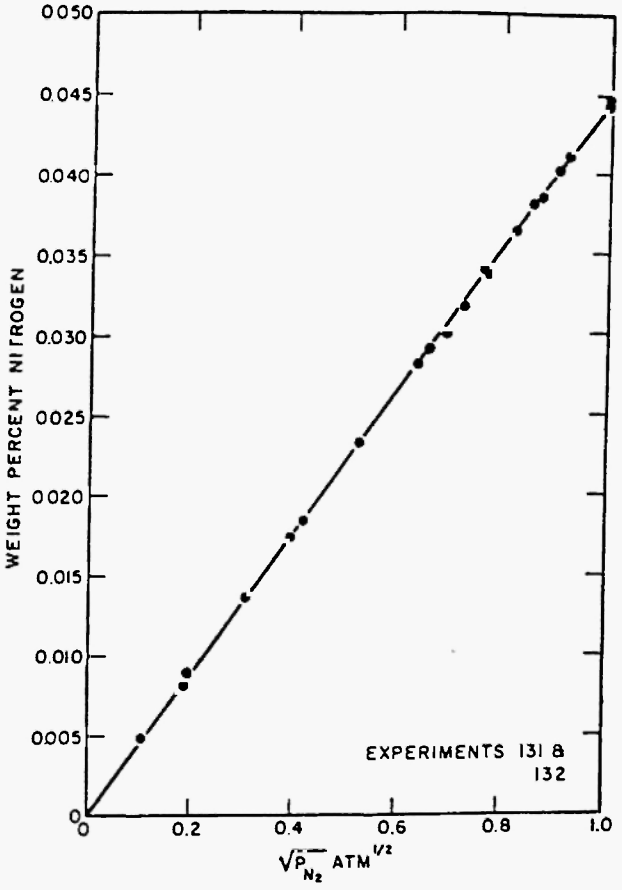

Fig. 1: Adherence to Sieverts' law by nitrogen in pure iron at 1606°C (after Pehlke and Elliott /3/)

$8x10^{-6}$ % N/°C. In general, the solubility can be written as follows, where T is temperature in Kelvin:

$$\log(\%N) = -\frac{188}{T} - 1.25 \quad (6)$$

Pehlke and Elliott /3/ also investigated the effects of numerous alloying elements on nitrogen solubility, and measured the interaction coefficients with nitrogen of each element. Nitrogen solubility is decreased by the presence of Al, C, Co, Cu, Ni, O and Si, while it is increased when Cr, Cb, Mn, Mo, Ta, W, and V are present, as summarized in Figure 2a. The effect on nitrogen activity is illustrated in 2b.

Another important study by Humbert and Elliot /5/ documents nitrogen solubility in pure iron, chromium and nickel, and varying compositions of their binary and ternary alloys at temperatures between 1500°C and 1800°C. This study is particularly significant because of the somewhat lesser volume of thermodynamic information available on nitrogen in nickel alloys. Values for solubility in pure iron at 1600°C were in agreement with those obtained by Pehlke and Elliott /3/, while it was determined that there is a small but finite solubility of nitrogen in pure nickel, of 0.001 wt % N at 1 atm pressure, a value unfortunately within the range of uncertainty for the experimental system. Chromium has an extremely high nitrogen solubility of 6.5 wt % in a supercooled liquid at 1600°C. The determination of solubilities in the binary and ternary systems was quite successful, as illustrated in Figures 3 and 4. It was observed that nitrogen obeys Sieverts' law in the ternary field up to approximately 50 wt % Cr. It is also to be noted from Figure 3 that there is a very large difference

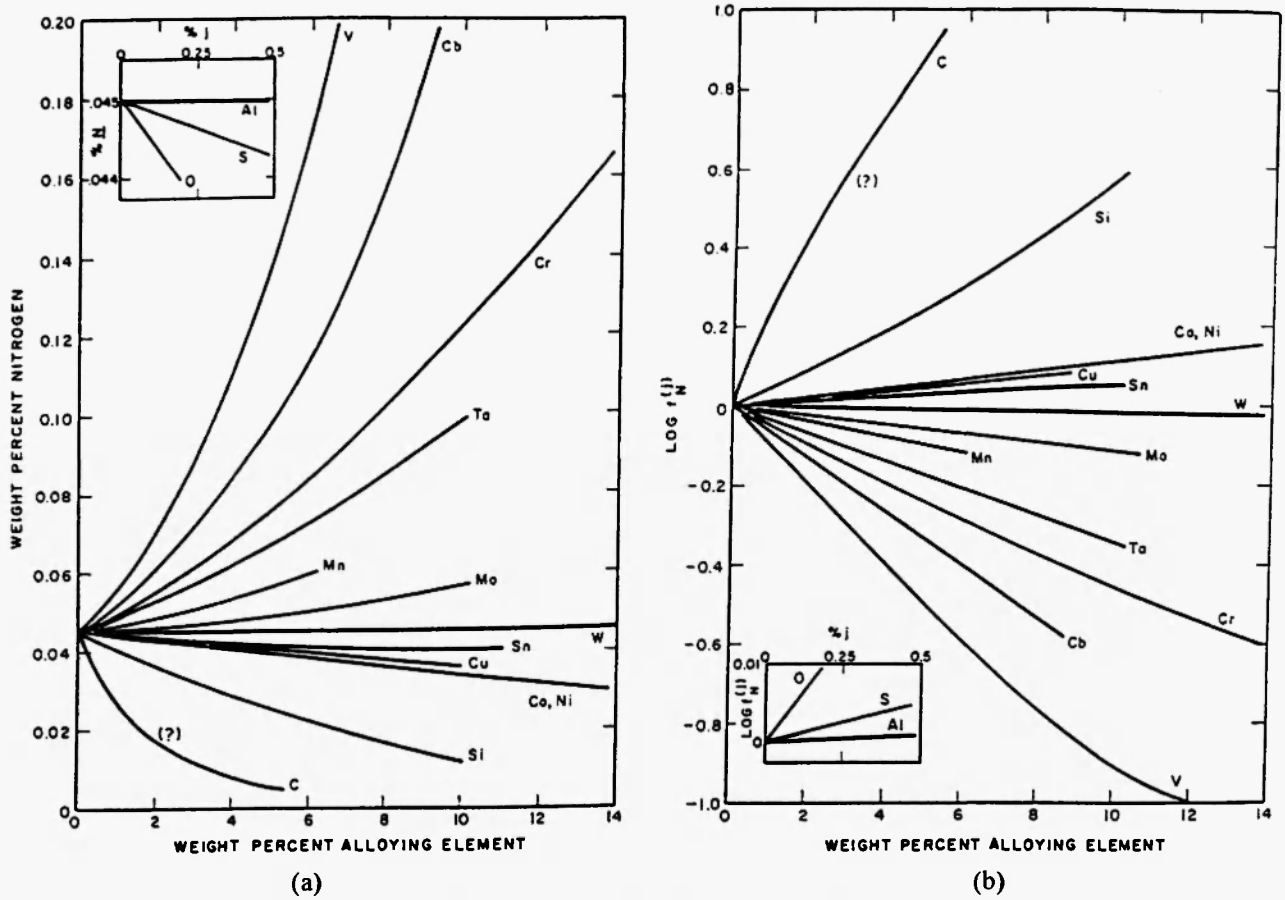

Fig. 2: **a)** Summary of solubility of nitrogen in binary liquid Fe–j alloys at 1600°C and 1 atm nitrogen pressure (after Pehlke and Elliott /3/) **b)** Effect of alloying elements on activity coefficient of nitrogen in binary Fe–j alloys at 1600°C and 1 atm nitrogen pressure (after Pehlke and Elliott /3/)

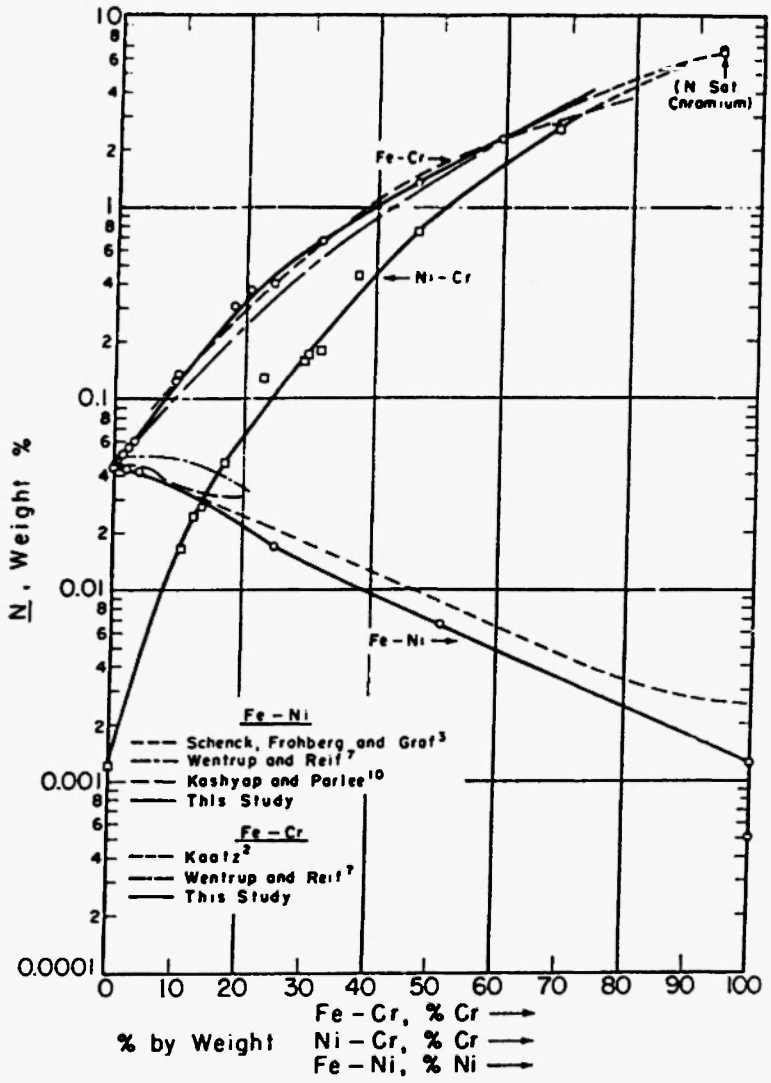

Fig. 3: Solubility of nitrogen in liquid Fe-Ni, Fe-Cr and Ni-Cr alloys at 1600°C and 1 atm nitrogen pressure (after Humbert and Elliott /5/)

between the solubilities of nitrogen in Fe, Ni and Cr. This factor is an important feature of the processing of the different alloys in the ternary systems, leading generally to very low specification levels of nitrogen in nickel-base alloys as compared with alloys that are essentially iron-based and have high chromium contents.

Naturally of interest following the fundamental solubility studies in Fe-Cr-Ni is the effect of titanium on solubility in such systems. Titanium is added to many steels as well as being present in most nickel base superalloys, and knowledge of its effects is extremely useful, as will be discussed below. Wada and Pehlke /6/ studied nitrogen solution and titanium nitride precipitation in dilute Ti-containing Fe-Cr-Ni solutions, and observed that nitrogen solubility follows Sieverts' Law up to a "break-point" nitrogen pressure, where the solubility suddenly increases. Shahapurkar and Small /7/ observe that this break point is consistent with the appearance of a second phase at the melt surface. This second phase is pure, stoichiometric titanium nitride. Figure 5 shows typical solubility data for an alloy similar to Incoloy 800 with 0.10% Ti, similar in shape to the curves of Wada and Pehlke /6/. However, while

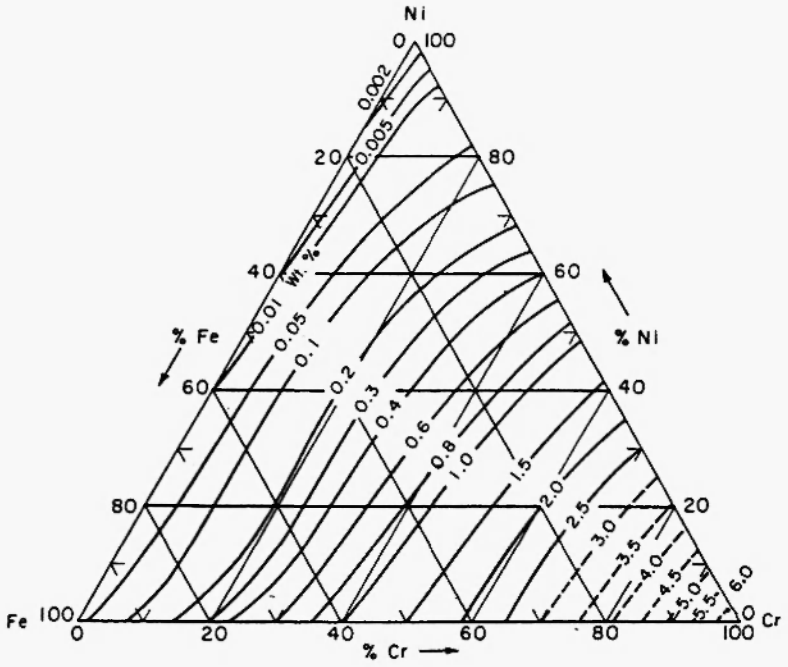

Fig. 4: Solubility of nitrogen in Fe-Cr-Ni alloys at 1600°C and 1 atm nitrogen pressure (after Humbert and Elliott /5/)

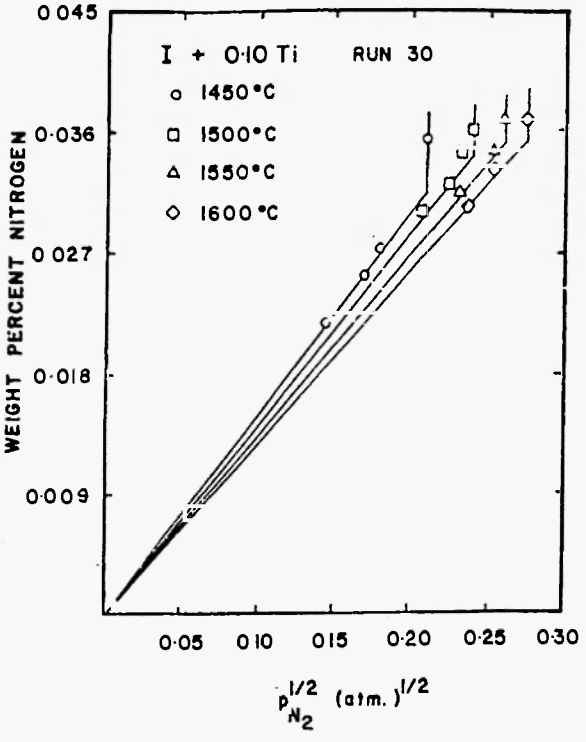

Fig. 5: Nitrogen solubility in an Fe-Cr-Ni alloy containing 0.10 % titanium (after Shahapurkar and Small /7/)

Wada and Pehlke /6/ observe that solubility of nitrogen in the alloys studied tends to increase with rising titanium level, Shahapurkar and Small /7/ note a decline in solubility, which they attribute to a decline in chromium activity with additional titanium, since it has been shown /3/ that chromium increases nitrogen solubility. The true trend remains somewhat unclear at this time, but a larger body of work tends to support an increase in solubility with Ti content. The absolute effect of Ti on nitrogen solubility is modified by the alloy base composition. When the alloy is predominantly a nickel-base system, the level of nitrogen at which TiN is precipitated is much lower than in the Fe-Cr systems.

An interpretation of established solubility data such as is presented above is given by Saito /8/ in terms of statistical thermodynamics. The interpretation is based on the fundamental concept that molten iron has a quasi-crystalline structure at temperatures slightly higher than the melting point, and in general, nitrogen atoms are not as randomly situated at lattice interstices to the extent that they are in the solid state. Rather, their distribution is dependent on the interaction energy U_{AB}

between the nitrogen atoms and atoms of other elements present in the alloy. For example, nitrogen atoms tend to cluster around Cr and Mn in molten Fe-Cr and Fe-Mn alloys. Based on interaction parameters calculated using this liquid model, the solubility in a multi-component alloy can be approximated in thermodynamic terms.

SOLUBILITY OF NITRIDES

As indicated above, titanium is a strong nitride former, even in dilute solution, and is often added to steels for nitrogen stabilization. Titanium is also present in minor amounts in most nickel-based superalloys, where it also has a strong tendency for nitride formation. Other nitride formers with behaviour paralleling Ti are Zr and Hf, also present in many superalloys and specialty steels. Due to the severe effect of titanium and other (Al, V, Cr, Nb,) nitride precipitates on the mechanical properties, it is of interest to control them through a fundamental understanding of the thermodynamic conditions under which they will form. The topic of inclusion removal by physical means will be treated below. While the following general discussion of solubility product will be given in terms of TiN, it should be noted that it is also applicable to other nitride formers.

The formation or dissolution of titanium nitride in a steel or superalloy can be represented by the following reaction,

$$TiN\ (s) = [Ti] + [N] \qquad (7)$$

while its equilibrium solubility product is defined as

$$K_s = [\%Ti \times f_{Ti}][\%N \times f_N] \qquad (8)$$

where f_{Ti} and f_n are the Henrian activity coefficients of Ti and N respectively. The equation exhibits a dependence such that if temperature is increased, the equilibrium shifts to the right as shown in Figure 6 /9/. If the solute contents of the dissolved elements are low, the mass concentrations of dissolved elements can be used to represent the solubility product, such that

$$K_s' = [\%Ti\ ][\%N] \qquad (9)$$

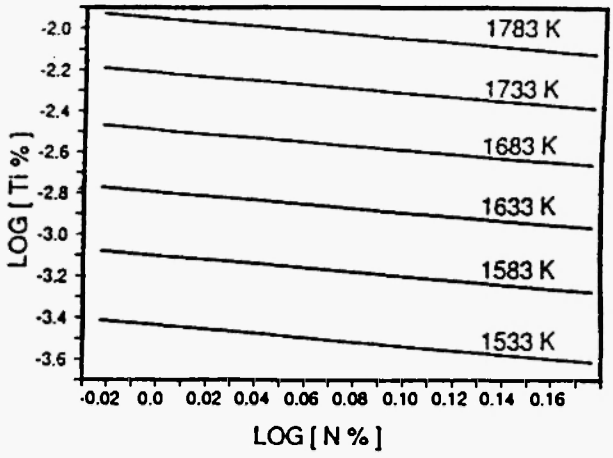

Fig. 6: Temperature and composition dependence of the TiN saturation solubility (after Mitchell /13/)

This modified solubility product is valid only where thermodynamic interaction coefficients can be ignored, which is often not the case. As seen in Figure 2b, the presence of any of several elements in iron will dramatically affect the nitrogen activity, and it has also been shown that chromium has a similar effect in superalloys /10/.

Liao and Fruehan /11/ studied the thermodynamics of Al and Ti inclusion formation in stainless steel and nickel alloys by measuring the activities of Al and Ti at low concentrations, and determining the equilibrium between metal, gas and nitride at different temperatures. The data was then used to construct inclusion stability diagrams to predict the occurrence of inclusion formation in the liquid bath. A sample stability diagram for TiN formation in Fe-18Cr-8Ni is shown in Figure 7 /11/. The curves represent the different solubilities of TiN in the melt at different temperatures. When the melt is cooled from the higher to the lower temperature at a specific composition, TiN will begin to form, and the composition of the melt will change along the line AB (due to the precipitation) as shown in the diagram, the slope of which is the ratio of atomic masses of Ti and N. It is then possible to calculate the total amount of TiN inclusions present for the system. Ozturk *et al.* /12/ constructed similar diagrams and compared the calculated values with inclusions found in industrial samples with good agreement.

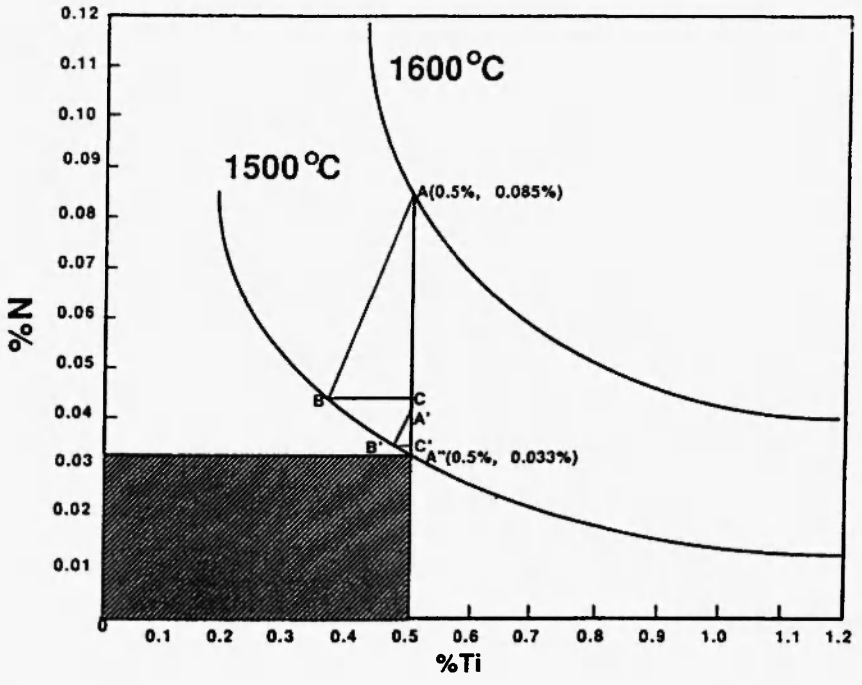

Fig. 7: Stability diagram for TiN in Fe-18Cr-8Ni at 1600 and 1500°C (after Liao and Fruehan /11/)

Nitride inclusions that are present in the liquid have a probability of contacting a refractory surface due to metal flow in several of the special melting processes. The most general case is that of pouring through a nozzle, for example at the exit of a tundish in the vacuum induction melting process. Since the balance of interfacial forces at such a surface leads to the nitride particle adhering to the refractory surface, the inclusions progressively build up at the interface (Figure 8). The clusters so formed may not only interrupt the casting process, but rather more seriously can break away from the surface at random intervals and produce inclusion clusters in the product of a size range much bigger than that of the individual particles. Defects due to this cause are frequently found in VIM material such as master alloy sticks, remelt electrodes and powder-atomised products (Figure 9).

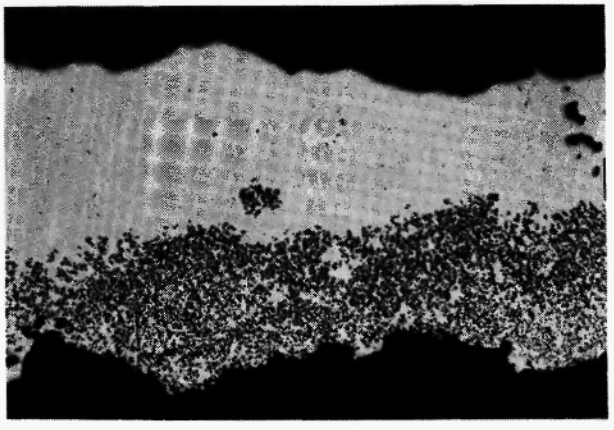

Fig. 8: Accumulation of nitride inclusion clusters on tundish exit nozzle walls following vacuum induction melting of Waspalloy (44x magnification)

It should be noted that TiN or other precipitates will also likely form during solidification due to the strong interdendritic segregation of solute elements /9/. This precipitation can be described by a combination of the temperature dependence of the solubility product and the temperature dependence of solute enrichment. If the solidification has been characterized by relationship between temperature and melt fraction solidified, then the temperature dependence of composition can be expressed by

$$C_L = C_0(1 - f_s)^{k_0 - 1} \qquad (10)$$

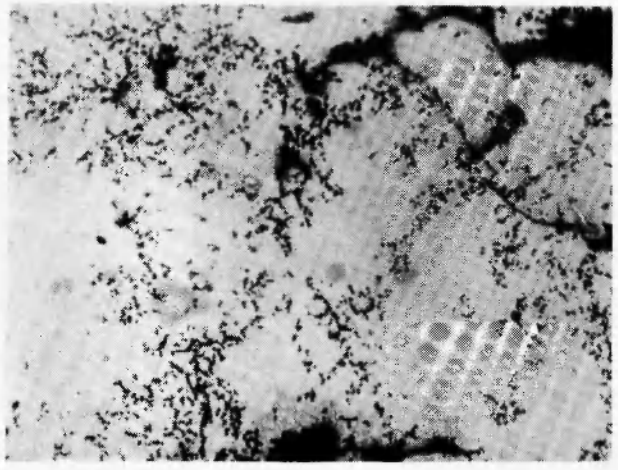

(a)

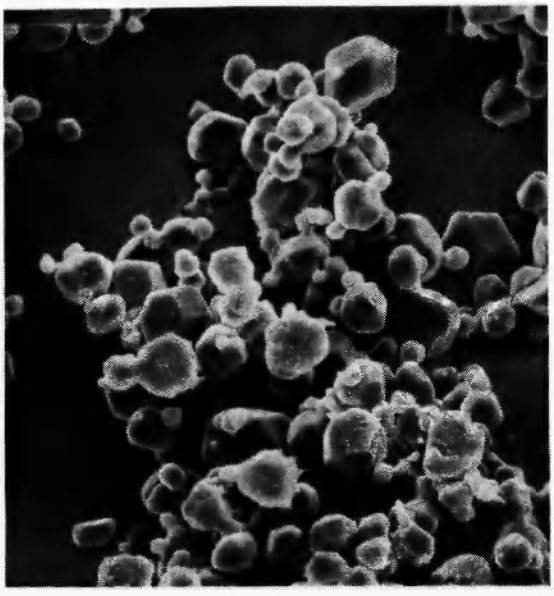

(b)

Fig. 9: Nitride inclusion defect in a product of vacuum induction melting a) flat, polished sample (1000x) and b) deep etched (1000x)

where C_L is the liquid composition, C_0 is the initial composition, f_S is the fraction solidified, and k_0 is the equilibrium partition coefficient. Cockcroft *et al.* /9/ made the calculation for IN718 with an interest in the effect of TiN formation on carbide precipitation, the result of which is shown in Figure 10. (It is to be noted that TiN is isomorphous with the MC carbides, such as NbC, and also with MN nitrides such as NbN and HfN,

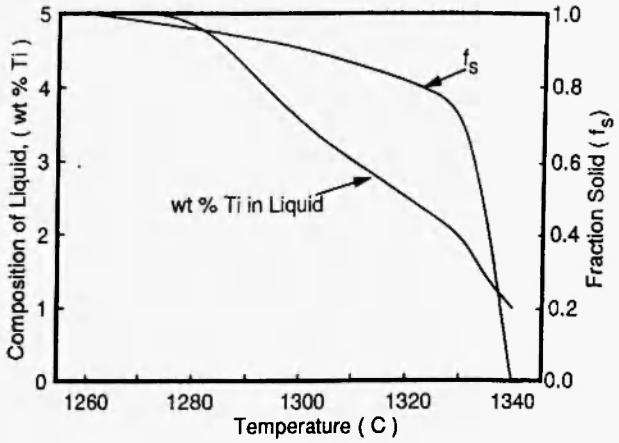

Fig. 10: Temperature dependence of interdendritic segregation of titanium and fraction solidified in IN 718 (after Cockcroft *et al.* /9/)

and can form continuous solid solutions with all of these compounds, leading to precipitates with sequentially-changing composition following the segregation processes, as shown in Figure 11). In any case, it is clear that the combination of temperature and concentration effects renders pure TiN almost completely insoluble in the alloy. The presence of TiN should go to zero only when the nitrogen content is less than the TiN saturation solubility, and it is suggested /13/ that even then the

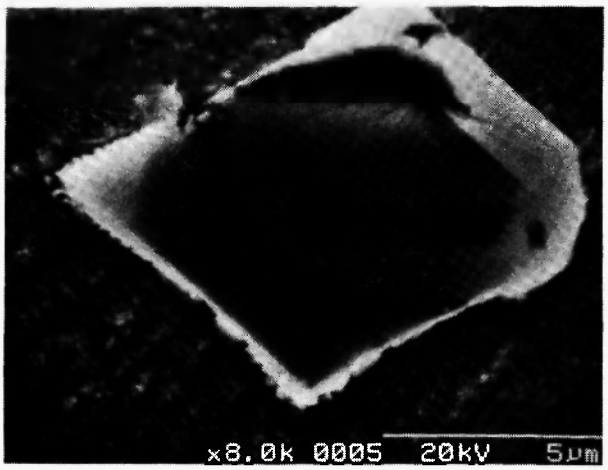

Fig. 11: 8000x magnification of a carbo-nitride precipitate structure in IN 718. An $MgO{\cdot}Al_2O_3$ hexagonally faceted core is surrounded by TiN, which provided a nucleation site for a primary MC carbide.

coarse dendritic nature of solidification in superalloys and the high extent of interdendritic flow will not entirely prevent TiN precipitation and agglomeration in the interdendritic regions. Rather, it is suggested that the nitrogen content be such that precipitation is suppressed until later in the solidification sequence, so that the precipitates may keep their role as nucleation sites for carbide precipitation but avoid growth and coalescence. In any case, if the alloy is processed at an elevated temperature, the solubility will be higher (equation (6) for iron) and the excess dissolved nitrogen will precipitate out upon cooling. As such it is imperative to use the minimum processing temperature possible, regardless of the processing route /13/.

Nitride precipitation is also a concern during the continuous casting of steel, when precipitation during the later stages of solidification may cause transverse cracking during the straightening process /14/. Turkdogan /14/ undertook a comprehensive review of this phenomenon for the case of HSLA steels, where it is found that strain induced precipitation of AlN and niobium and vanadium carbonitrides are responsible for low hot ductility, increasing the crack-sensitivity of the steel. However, if the steel is treated with titanium, TiN precipitates in the interdendritic zones during solidification, shown in Figure 12, and is accompanied by interdendritic segregation of other alloying elements (Al, Nb, V, C) that do not necessarily precipitate during freezing. Rather, they nucleate and grow as carbides on the TiN during cooling, resulting in coarse precipitates. The coarse precipitates do not affect the hot ductility of the steel, and no transverse cracking is observed. In order to ensure sufficient coarsening of the precipitates, it is suggested that the nitrogen level is kept low (<60 ppm) and a corresponding amount of titanium be added for a fine dispersion of TiN /14/.

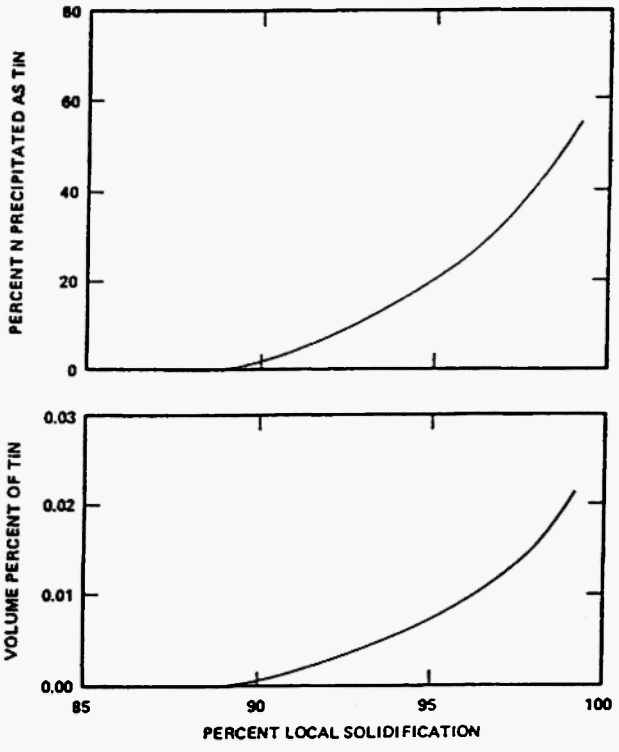

Fig. 12: Calculated TiN interdendritic liquid precipitation during solidification of steel containing 0.02% Ti and 60 ppm N (after Turkdogan /14/)

KINETICS OF NITROGEN ABSORPTION AND DESORPTION

A number of models for nitrogen absorption and desorption to and from liquid metals have been put forward. The information available in the literature is either inconclusive or conflicting, which may stem from the fact that it is seldom that sufficient information is provided by a single kinetic study to establish a mechanism, as noted by Belton /15/. Consequently, a large body of work is available in the literature on the topic, and for an extensive review the reader is referred to Battle and Pehlke, 1986 /16/. The reported possible approaches for the characterization of liquid metal/nitrogen reactions are summarized below.

Equation (1) introduced the overall reaction for nitrogen adsorption. This reaction can be broken down into 5 kinetic steps as follows, any one of which may become rate controlling /17/:

1. Transport of nitrogen gas molecules through the bulk gas phase to the vicinity of the gas-metal phase boundary.
2. Transfer of nitrogen molecules through the gas boundary layer.
3. Adsorption at the interface, followed by the chemical dissociation reaction of nitrogen molecules.

4. Transport of atomic nitrogen through the boundary layer in the metal on the concentration gradient.
5. Transport of atomic nitrogen in the bulk liquid metal phase by diffusion and convection.

For adsorption studies on high purity iron, it is almost invariably found /16/ that concentration-time data is characterized by integration of a standard first order rate equation:

$$\frac{dC}{dt} = k\frac{A}{V}(C_e - C) \qquad (11)$$

where A is the exposed surface area, C is the melt concentration at time t, k is the first order mass transfer coefficient, V is the bath volume, and C_e is the equilibrium melt concentration. Desorption is better described by integration of a second order equation:

$$\frac{dC}{dt} = k'\frac{A}{V}(C_e^2 - C^2) \qquad (12)$$

where all values are as previously defined except for k', the second order rate constant. Several researchers have evaluated k and k' within reasonable agreement. Values for k range from 19 to 35 x 10^{-3} cm/s, while k' ranges from 62 to 693 cm^4/s mol /14/. Reaction rates increase with temperature, and absorption increases with nitrogen pressure, as shown in Figures 13 a) and b) from Rao and Lee /4/. However, reaction rates and rate constants both decrease significantly with addition of elements such as oxygen and sulfur that are surface active. Fruehan and Martonik /18/ have shown conclusively that the overall reaction changes to second order, and becomes strongly dependent on the concentration of such elements. As a result, elements that increase reaction rate tend to be deoxidizers. Models developed to explain such characteristics are numerous and the reader is again referred to Battle and Pehlke /16/, who provide an exhaustive compilation of kinetic models. Three steps are examined in some detail here.

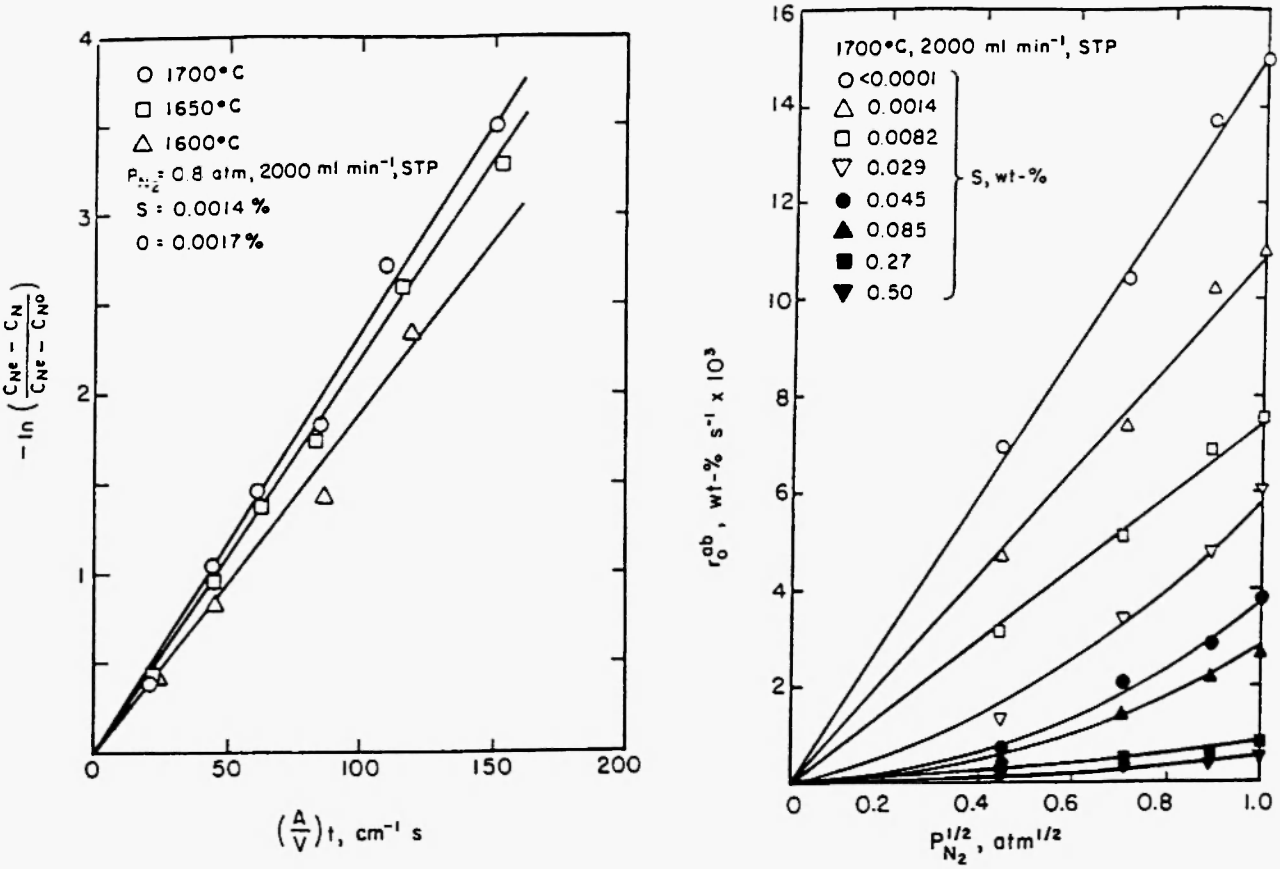

Fig. 13: a) Effect of temperature on nitrogen absorption in liquid iron (after Rao and Lee /4/)
b) Effect of nitrogen partial pressure on initial rate of nitrogen absorption (after Rao and Lee /4/)

Gas Phase Mass Transfer

In general, if the process of gas-phase mass transfer is rate controlling, the rate can be written as follows:

$$\frac{dC}{dt} = \frac{k_g A}{RT}(p_{N_2} - P_{N_2 i}) \qquad (13)$$

where C is the nitrogen concentration at time t, k_g is the gas phase mass transfer coefficient, R is the gas constant, A is the surface contact area, T is the film temperature, and the last term is the difference between the bulk nitrogen pressure and that at the interface. Gas phase mass transfer appears to be limiting for desorption into an inert atmosphere, as illustrated by Choh *et al.* /19/.

Interfacial Chemical Reaction

There is evidence to suggest that the general chemical reaction at the interface may significantly affect nitrogen reaction rates, particularly for the case of high concentrations of surface-active elements where the reaction is second order, and appears to be controlled by the dissociation of the nitrogen molecule /18/. Since oxygen and sulfur are almost invariably present in liquid steel, the effects of these solutes are of practical interest. While intrinsic reaction kinetics are generally difficult to measure, some successful work has been done using the isotope exchange method, which permits a direct determination of the N_2 dissociation rate on the metal surface by the reaction

$$^{28}N_2 + {}^{30}N_2 = 2\,{}^{29}N_2 \qquad (14)$$

while eliminating the effects of liquid phase mass transfer. Studies of this type have been performed by Byrne and Belton /20/, Kobyashi *et al.* /21/, and Glaws and Fruehan /22/. Notably, Byrne and Belton /20/ determined the first order rate constant as a function of temperature for the dissociation of nitrogen on pure iron, and the apparent rate constants as a function of sulfur activity at several temperatures. In addition, they compared their results with other studies (see Figure 14) that had been corrected for the effect of mass transfer, and found good agreement, indicating that nitrogen

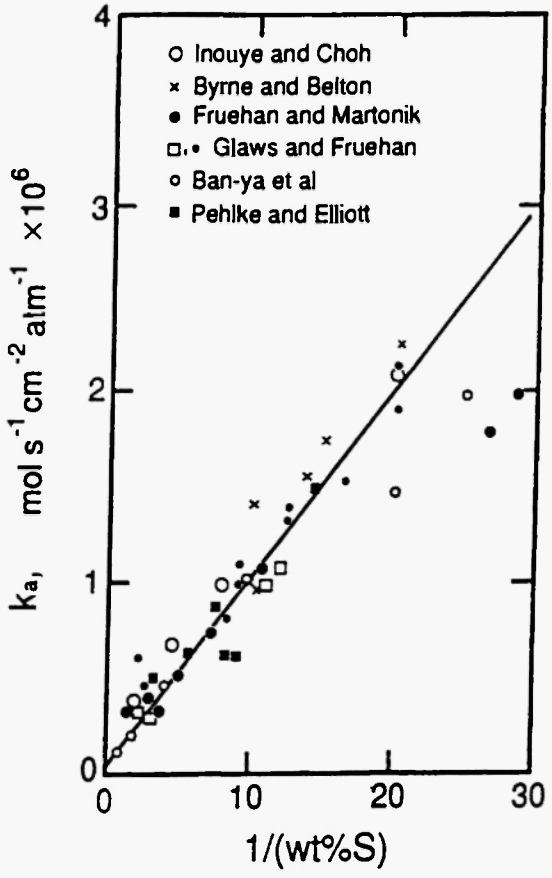

Fig. 14: Apparent first order rate constants for absorption of nitrogen into liquid iron at 1600°C as a function of sulfur content (after Byrne and Belton /20/)

absorption rate is controlled by dissociative chemisorption of nitrogen.

Belton /23/ also provides a comprehensive study of reaction site blockage by surfactive elements. If ideal adsorption is assumed, the fractional solute coverage, θ, can be defined by equating the Gibbs adsorption isotherm, in which surface tension is related to solute activity, to the Langmuir isotherm which relates activity to surface coverage. If sufficient surface data is available, the adsorption coefficient K_a can then be described by

$$\frac{\theta}{1-\theta} = K_a a_s \qquad (15)$$

where a_s is the solute activity. Assuming reaction rate k

is directly proportional to surface coverage, as θ approaches unity,

$$k = k_{bs} / K_a a_s \tag{16}$$

where k_{bs} is the reaction rate constant for a bare surface. Belton /23/ found evidence to support this result for surface coverages above 0.6. Finally, the rate equation is given as

$$\frac{dC}{dt} = \frac{A}{V}\left(\frac{k_{bs}K_a}{a_s}\right)p_{N_2} \tag{17}$$

where all variables have their previous definitions.

While much work has been done regarding the effects of surfactive elements on nitrogen absorption by liquid iron, only one recent (1995) study by Ono *et al.* /24/, examines the effect of non-surface alloying elements including Ti, Zr, V and Cr, all of which have stronger affinities for nitrogen than iron. It was found that the rate of nitrogen dissolution into the liquid metal increases linearly by addition of these metals as shown in Figure 15. Titanium particularly increases the reaction rate, with 0.08 wt % Ti increasing the rate constant for pure iron by 1.5 times. It is postulated that these elements change the energetics of nitrogen adsorption by increasing the activity of vacant sites at the metal surface. The two principal factors in controlling the absorption site fraction in liquid alloys are the contents of sulphur and oxygen respectively, both of which are more strongly surface active than nitrogen /25/. In the context of special melting techniques, it is unlikely that sulphur would be present at levels strongly affecting the nitrogen absorption process, but oxygen is normally present in the concentration range required to affect absorption. Experimental results and industrial observations on this point are difficult to interpret since the oxygen content is normally controlled by the presence of de-oxidising elements such as Ti and Al which also have an intrinsic effect on nitrogen behaviour through modification of the nitrogen activity coefficient in solution. However, it is observed that when magnesium is added to liquid nickel-base alloys, the nitrogen removal rate is considerably enhanced when the Mg content of the bath exceeds 200 – 300 ppm. In principle, the same result ought to be obtained with Ca additions to iron-base alloys, but no observations of this nature are reported.

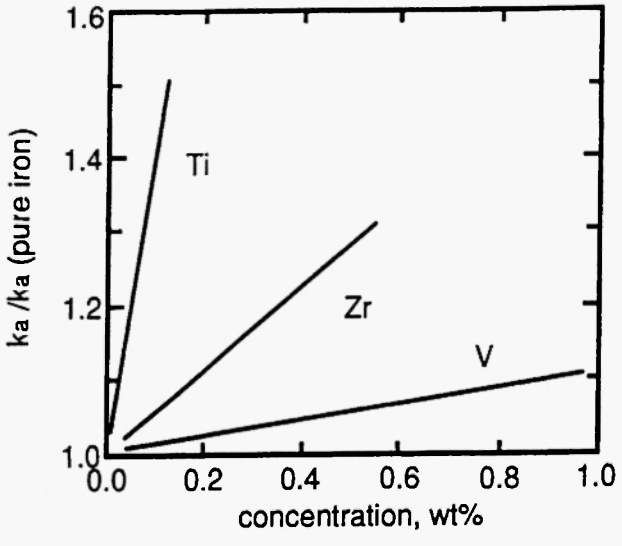

Fig. 15: Effect of added elements on the rate constant of nitrogen dissolution (after Ono *et al.* /24/)

Liquid Phase Mass Transfer

Transport in the liquid phase is generally not assumed to be rate controlling, since many processes involve inductive stirring, but if it is, it is generally expected that a first order reaction with respect to nitrogen concentration will prevail, according to equation (11). The integrated form gives the concentration C at time t as

$$\ln\left(\frac{C - C^e}{C^o - C^e}\right) - k_m \frac{A}{V} t \frac{C^o}{C^o - C^e} \tag{18}$$

where C^o is the initial nitrogen concentration and k_m is the liquid phase mass transfer coefficient. As indicated above, this equation holds for absorption in pure metals with low surfactive concentrations /17/.

The model which has most generally been used for prediction of liquid-phase mass transfer rates in vacuum induction melting is that of Machlin /26/, who proposed that the process could be represented by a scheme in which small volume elements of liquid were placed at the centre surface and at the bulk concentration. They were then transferred across the surface at the liquid bulk velocity without mixing with the bulk liquid,

during which time they transferred material to a surface reaction (e.g. an evaporative process, or gas desorption) by liquid diffusion. The model has proved quite accurate in the prediction of evaporation rates when used in conjunction with practical observations of surface velocity, and would presumably be equally successful in predicting nitrogen desorption rates from a surface, providing that the state of the surface with respect to oxygen contamination was known. More recent CFD models of fluid flow in the vacuum induction crucible /27/ have led to very similar results in respect of the evaporative process and would remove the need for experimental measurement of the surface velocity in order to predict gas desorption rates. It is clear, however, that the desorption process in industrial superalloy compositions and in highly alloyed steels melted in vacuum systems of 1 – 5 Pa is extremely slow, of the order of 5 ppm N / hr, and this mechanism is therefore not a viable technique for achieving large reductions in nitrogen contents. Also, since the rate is probably controlled by the surface oxygen content, reducing the vacuum pressure would have no effect on the overall rate unless the system were held in a container other than an oxide crucible, since decomposition of the oxide controls the oxygen potential of the conventional system.

MEANS OF NITROGEN CONTROL

Vacuum Induction Melting (VIM)

Sieverts' Law (equation (4)) describes the dependence of solubility on nitrogen partial pressure, and suggests that melt treatment in vacuum might be an effective means of nitrogen removal. Unfortunately, however, kinetics rather than thermodynamics often determine the degree of refinement in vacuum /26/. In metals and alloys not containing strong nitride formers, nitrogen removal at 0.5 to 2 Pa can be achieved, although slowly (see above), but chromium steels for example show a discrepancy of more than an order of magnitude between equilibrium and observed nitrogen levels /28/. This is due to a strong affinity of nitrogen for chromium and other elements that reduce the nitrogen activity and so the removal rate, ultimately generating a lower limit for removal that increases with Cr content at any given pressure. Theoretically, if a melt is given sufficiently long exposure to a pressure of less than 0.01Pa, an ultra low nitrogen content should be attainable, but the necessary processing times are generally too extensive for commercial operation /29/. The extremely low partial pressures required also impose a severe equipment restriction /13/. It should also be noted that until all solid nitrides such as TiN are removed, pressure will not affect removal rates /30/.

Some key factors arose from a study by Simkovich /31/ of variables affecting nitrogen removal from iron and nickel base alloys under reduced pressure including composition, temperature and exposure time. The initial vacuum exposure of iron and nickel base alloys with high nitrogen concentrations relative to the saturation limit at the particular pressure is accompanied by a rapid release of nitrogen, followed by slow removal at a decreasing rate, shown in Figure 16 for two alloys. It was also found that alloys containing aluminum, columbium or titanium retain significantly higher residual nitrogen than the same alloys without such elements, however this result was not observed for the case of chromium. A comparison of experimental results with industrial VIM data for several alloys, including superalloys IN600 and IN718, yielded similar reaction rates, even considering different surface to volume ratios. This indicates that removal of nitrogen from iron or nickel base bath is not controlled by liquid phase diffusion, but more likely by adsorption of the nitrogen on the metal surface as discussed above.

During VIM it has been noted /32/ that the quick initial nitrogen removal rate upon exposure to vacuum is often accompanied and augmented by the so-called carbon-boil, which is also pressure dependent. This reaction is;

$$[C] + [O] = (CO)\,(g) \qquad (19)$$

where dissolved carbon and oxygen in the melt react to nucleate CO gas bubbles. These bubbles provide areas of local low partial pressures within the melt (although the melt is under vacuum, the ferrostatic head rapidly increases the pressure with depth penetration into the melt). To satisfy Sieverts' Law nitrogen then diffuses into the bubbles, which also reduce diffusion distances and increase metal-gas interface area /33/. For a more

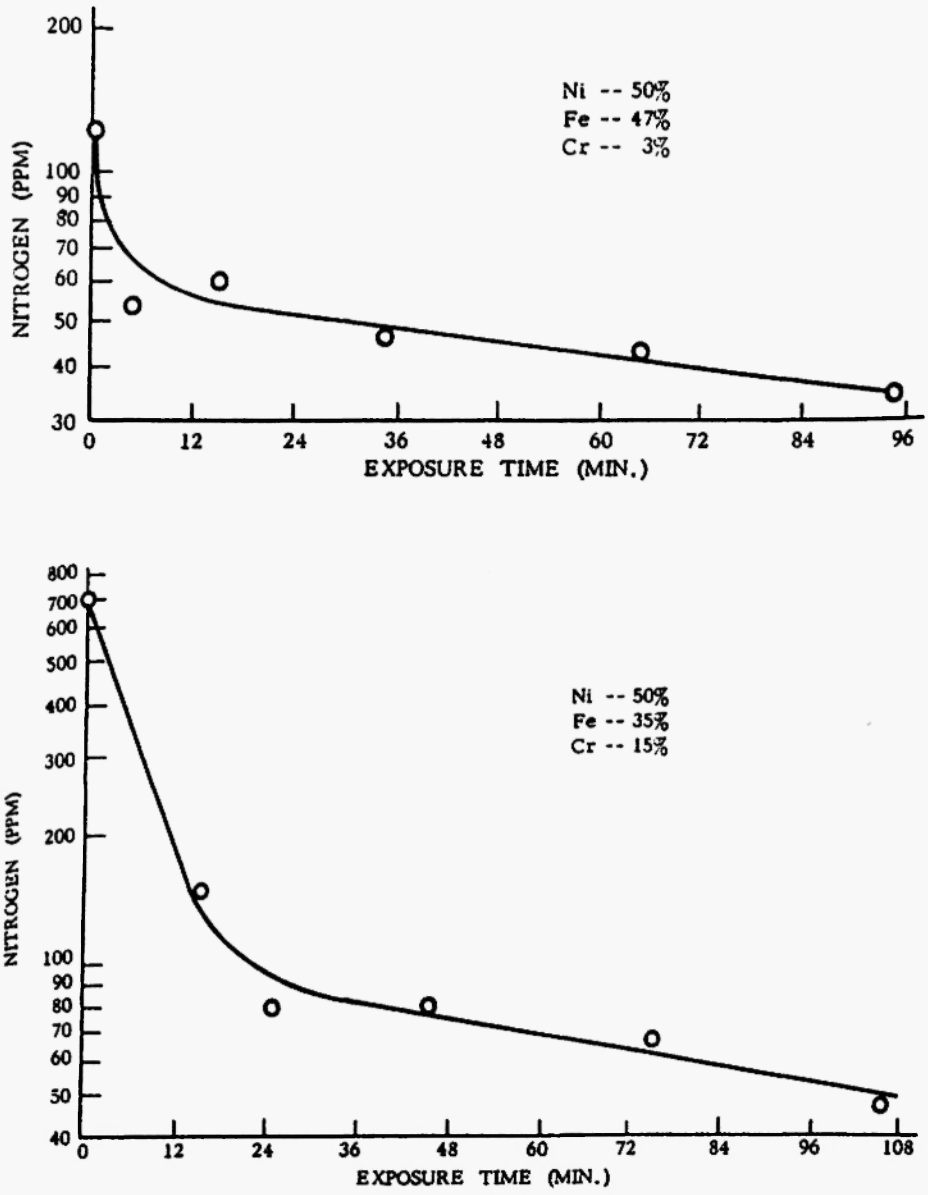

Fig. 16: Relation between nitrogen content and exposure time at 2800°F and a chamber pressure of 5 microns (after Simkovich /31/)

complete description of the carbon boil and the associated kinetic model based on fluid flow, the reader is referred to Machlin /26/. This process, however, also has thermochemical limitations. Nitrogen will only diffuse into the CO bubbles following the chemical potential gradient and this driving force decreases as the partial pressure builds up within the bubble. Since the equilibrium partial pressure of nitrogen for liquid-phase contents of the order of 20 ppm is approximately 1Pa, the process will cease when the gas in the bubble contains approximately 1 ppm of nitrogen. Obviously, then, a very large flow of CO bubbles would be required to remove a significant amount of nitrogen. The same principles apply to the use of argon bubbling in the VIM furnace also for the purpose of removing nitrogen.

While a small amount of nitrogen control can be achieved by adherence of insoluble nitrides (TiN, ZrN) to crucible walls, or addition of slag-making flux to

entrain them, nitrogen is best controlled in the VIM process through a combined use of low operating pressure and low-nitrogen raw materials /29/. Katayama and Nakamura /34/ developed a process for production of ultra-low-nitrogen alloys via a two-step process; first denitriding solid state raw materials with Mg-$MgCl_2$ flux in a closed vessel, and then conventional VIM to prevent re-absorption. Data is presented which indicates an average of 8 ppm residual nitrogen for stainless steel, Cr alloys and plain carbon steels. However, the process is limited by the size of the charge materials and may have limited industrial use.

Precipitation and Filtration

While it may not be economical to remove nitrogen through long exposure times to vacuum, in some cases it may be acceptable to remove some nitrogen from the alloy through solid nitrides that remain in the liquid metal after vacuum treatment /33/. Some of the reactions are

$2[Nb] + 2[N] = 2NbN$	$\Delta G^{\circ}_{298K} = -106$ kcal/mol
$2[Al] + 2[N] = 2AlN$	$\Delta G^{\circ}_{298K} = -113$ kcal/mol
$2[Ti] + 2[N] = 2TiN$	$\Delta G^{\circ}_{298K} = -147$ kcal/mol
$2[Zr] + 2[N] = 2ZrN$	$\Delta G^{\circ}_{298K} = -151$ kcal/mol

where the free energies can be used for comparison of stability. Bieber and Decker /33/ performed experiments on a nickel-iron–chromium alloy to illustrate the denitrifying power of the above elements. The cast alloy exhibited macroporosity that was reduced most significantly in decreasing order Ti, Zr, Nb, Al, Mg, consistent with the relationship between the standard free-energy values. Titanium was the preferred addition over Zr due to its greater solid solubility in that alloy system. It is to be noted that the carbides of the above elements are less stable than the nitrides in the alloy systems considered and are seldom found to be precipitated in the liquid state. However, the use of the elements as nitrogen "getters" is limited by the need to prevent undesired carbide precipitation in the final alloy.

Solid nitrides may be filtered out prior to, or during casting. Chen and co-workers /35/ investigated the mechanism of inclusion removal with a typical Al_2O_3-base foam ceramic filter, and determined that the removal process is the adsorption of particles on the filter surface due to a decrease in interfacial energy as compared with the inclusion/melt interface, i.e. essentially the same mechanism as that of nozzle accumulation described above. Once the particles come in contact with the filter walls, they become entrapped in the stagnant boundary layer, sinter to the filter and then agglomerate by attracting the same type of inclusions in the liquid metal. In the case of TiN inclusions, it appears that the agglomeration process is enhanced by the presence of alumina particles that act as a "glue" in holding together the TiN particles. The material, porosity and interior surface roughness all influence the filtration efficiency as is reported in the literature /36/. Filters with a porosity range of 10 – 20 ppi are commonly used during VIM, but filters with pore sizes down to 60 ppi have been used successfully during vacuum investment casting processes.

While such filtration is quite effective for the case of TiN, the particles must obviously be solid at the filtration temperature /37/. The main pitfall of the filtering process is the associated heat loss that must be compensated for with additional superheat /30/. Unfortunately, an increase in temperature increases the solubility of the TiN particles, which consequently lessens the effectiveness of the filtration process. Also, since the necessary temperature is higher than the liquidus, the limiting result of filtration is the nitrogen content in equilibrium with TiN at the filtration temperature /30/.

TiN has a bulk density that is approximately half that of a typical liquid superalloy and so some separation by simple flotation ought to be possible. However, the terminal velocity reached by the small inclusion particles is much less than the normal convection velocities in liquid metal processing and although a small fraction of the particles might be expected to reach a free surface, in practice there is a much greater probability that they will be trapped by collisions with the container refractory surfaces, or in the case of VAR/EB with the frozen skull on the mold wall. The interfacial forces operating on the free metal surface retain particles against bouyancy. This feature can be demonstrated in the case of HfN particles, which are more dense than liquid superalloys. In the EB button

melting technique /38/ for inclusion assessment, HfN particles are found to collect in the surface "raft" of inclusions where the density relationship should dictate that they would be found in the bulk of the alloy. (It may also be noted that in this case, the same mechanism holds true for HfC).

Vacuum Arc Remelting (VAR)

In the case of vacuum arc remelting (VAR), it has also been observed that attained nitrogen levels are higher than those predicted by thermodynamics /39/, although the small droplet size and low melting rates of this technique imply that there should be a close approach to equilibrium. Tommaney and Ramachandran /39/ postulate that this deviation can be derived from a consideration of both kinetics and the geometry of the VAR furnace, and they investigate nitrogen control during the process. It is determined that the most important variable is the nitrogen pressure directly above the pool of liquid metal, which depends upon gas content of the electrode, arc gap and melt rate, and that there is a pressure differential resulting from furnace geometry that prevents attainment of lower nitrogen levels. This result is illustrated in Figure 17. However, it is concluded that control can be accomplished by modification of equilibrium solubility calculations to accommodate such differences, although geometric

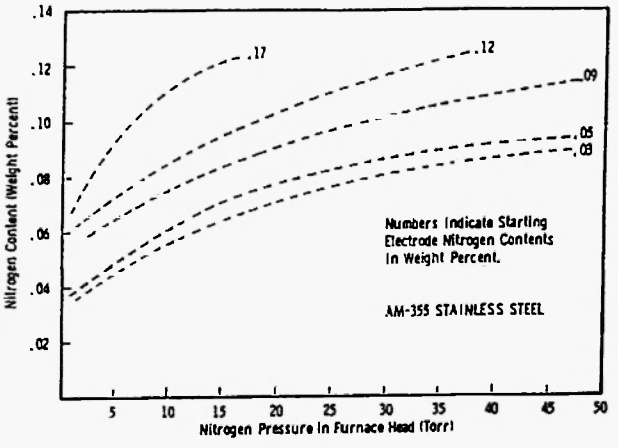

Fig. 17: Effect of electrode nitrogen content and furnace head pressure on the final nitrogen content of an ingot during VAR, also showing equilibrium solubility (after Tommaney and Ramachandran /39/)

considerations would dictate empirical determination of constants.

The metal being processed by VAR undergoes a temperature sequence in which it is heated to the melting point during the electrode feed into the arc region; maintained at high temperature during the liquid's passage through the arc region and ingot pool; then finally cooled through the freezing range in the ingot body. In principle, all nitrides should dissolve during the heating stage, up to their saturation solubility at the process temperature, and subsequently re-precipitate during the cooling process, both in the liquid and the solid. If this process operates, the nitride particle distribution in the final solid should be characteristic of the ingot temperature gradients/solidification rates, and would not be related to the nitride distribution in the starting electrode. The extent to which the foregoing scenario is correct depends on the melting rate of the electrode, and also on the maximum temperature attained by the liquid metal. The result depends also on the possibility for inclusion agglomeration to take place during the metal residence time in the liquid ingot pool, as has been demonstrated /40/. In the case where the nitrogen content is less than that at TiN saturation at the liquidus temperature, agglomeration does not take place. Some of the TiN particles which survive to the electrode liquid surface/vacuum interface are held there by surface tension forces and are to be found on the ingot liquid surface after the droplet transfer process. The particles are driven to the surface periphery by the flow regime of the pool and collect on the ingot surface. In an example ingot of IN718, with a bulk content of nitrogen of 80 ppm, the outer 5 mm of the VAR ingot was found to contain approximately 300 ppm nitrogen arising from this inclusion collection mechanism. A mass balance indicates that this mechanism accounts for approximately one-third of the nitrogen removal during the process.

In general during VAR and solidification the nitrogen removal from solution will be controlled by liquid phase mass transfer and evaporation kinetics. It is reported that /30/ for concentrations below 40 ppm mass transfer dominates and is controlled by fluid flow. Nitrogen content can be expected to decrease to about 80 ppm from an initial IN 718 ingot content of 100 ppm during VAR processing /30/. While the size and shape

of the liquid metal pool have some effect on nitrogen removal /41/ since TiN inclusions are collected at the pool boundaries, the main concerns for sufficient VAR nitrogen removal are essentially the same as for VIM; low nitrogen raw materials and removal of solid TiN at the liquidus temperature /30/.

Electroslag Remelting (ESR)

Electroslag remelting may also be used to provide a certain amount of nitrogen removal. In this case, TiN inclusions can be physically removed by entrainment in the slag, and by the surface collection mechanism described above. In addition, melts that do not contain strong nitride formers can also experience nitrogen removal, since ESR slags have a finite nitrogen capacity. Nitrogen dissolves in slags as either of

$$1/2\ N_2 + 3/2\ O^{2-} = N^{3-} + 3/4\ O_2 \qquad (20)$$

$$N_2 + C^{2-} = CN_2^{2-} \qquad (21)$$

depending on the carbon content of the system.

The first of these equations indicates that a more basic slag should have a higher solubility as seen in Figure 18 for the CaO-CaF_2 system as determined by Martinez *et al.* /42/. The nitride capacity of the slag C_N is then

$$C_N = \frac{(\%N)\cdot(P_{O_2})^{3/4}}{(P_{N_2})^{1/2}} \qquad (22)$$

It was also determined that a slag containing a metal with a strong affinity for nitrogen will have a higher nitrogen capacity., ie. B_sO_3 or Ti_2O_3 containing slags. The relevant equation is /15/:

$$M_xO_{1.5}(s) + 1/2\ N_2(g) = M_xN(s) + 3/4O_2(g)$$
$$x=1 \text{ for B, Al } x = ¾ \text{ for Si, Ti} \qquad (23)$$

The mechanism of this reaction was proposed to be incorporation of nitrogen into borate or titanate networks. Elissa *et al.* /43/ studied nitrogen behaviour during ESR of titanium- free tool steels, and claimed that 15 to 67% of initial electrode nitrogen content could be removed by ESR, and also that replacement of

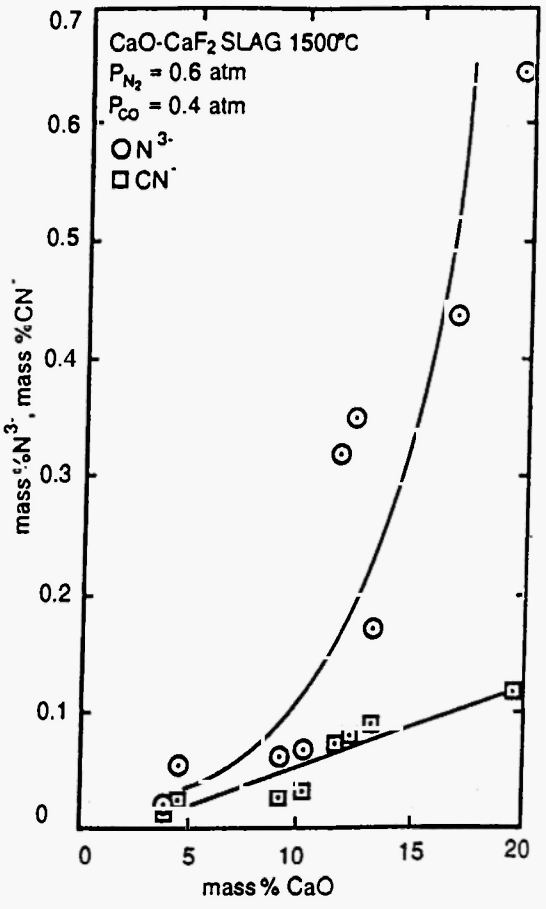

Fig. 18: Nitride and cyanide contents of CaO-CaF_2 slags as a function of CaO content at 1773K (after Martinez *et al.* /42/)

CaO by Al_2O_3 in the ESR flux increases viscosity with the result of higher denitrogenization.

In the case of titanium-containing superalloys, nitrogen behaviour during ESR is somewhat different from that observed in VIM or VAR, mainly due to the different nature of the oxide inclusions that played a role in nitride agglomeration during VIM and VAR /44/. In general, nitrides are less likely to agglomerate in ESR, even at high super-saturations, since the oxide inclusions are predominantly calcium aluminates having a lower melting range and with lower interfacial tensions against TiN. Another difference in the ESR system is the presence of an atmosphere as opposed to low pressure. Low (~20 ppm) initial nitrogen containing electrodes of a superalloy will experience nitrogen pickup during processing in air, since, for example, the

steady-state concentration of IN 718 ESR melted in air is around 60 ppm /44/. Thus for the very low range of alloy nitrogen concentrations, processing by ESR will require a protective atmosphere. Such techniques have been developed, but create additional practical problems for the ESR operation /44/.

ESR and a closely related process, Arc-Slag Melting (ASM) are used for the production of special high-nitrogen steels. The ESR version of the technique employs an ESR system that operates under an elevated pressure of nitrogen, which serves to retain a nitrogen addition made either to the electrode during a prior manufacturing step, or to retain a nitrogen content achieved by additions of silicon nitride during the ESR process. In both cases, the result is a steel which may contain up to 0.9% nitrogen, offering some interesting possibilities for the manufacture of austenitic stainless steels, modified martensitic alloys and tool steels /45/. The required pressure depends on the alloy's solidification mechanism as well as on the required nitrogen content. If the alloy solidifies austenitically, the nitrogen solubility increases with falling temperature, and the required pressure is determined by the nitrogen content specification. If the alloy solidifies to the delta phase, there is a sharp decrease of nitrogen solubility at the liquidus, and an overpressure of nitrogen is required to prevent microporosity (Figure 19). Pressures up to 2.5 MPa have been used, but the range of 0.5 – 1 MPa is more usual. The ESR process is conducted in the normal way and the final nitrogen content is predictable from Sieverts' Law applied to the alloy concerned.

The ASM process is based on the ESR concept, but employs a melting mode in which the electrode arcs directly into the slag surface, instead of being fully in contact with the slag. The process therefore contains the same slag-metal reactions and heat balance as ESR, but with the addition of the arc process at the slag surface, as shown schematically in Figure 20 /46/. The advantage from the point of view of high nitrogen steels is that the solidification parameters retain the good ESR characteristics, but the arc process produces a high degree of ionisation in the nitrogen atmosphere and therefore greatly enhances the rate of nitrogen pick-up into the alloy, in the same manner as is observed in plasma melting with nitrogen-based plasmas /47/, but at a much lower cost. It has been found /46/ that the rate of

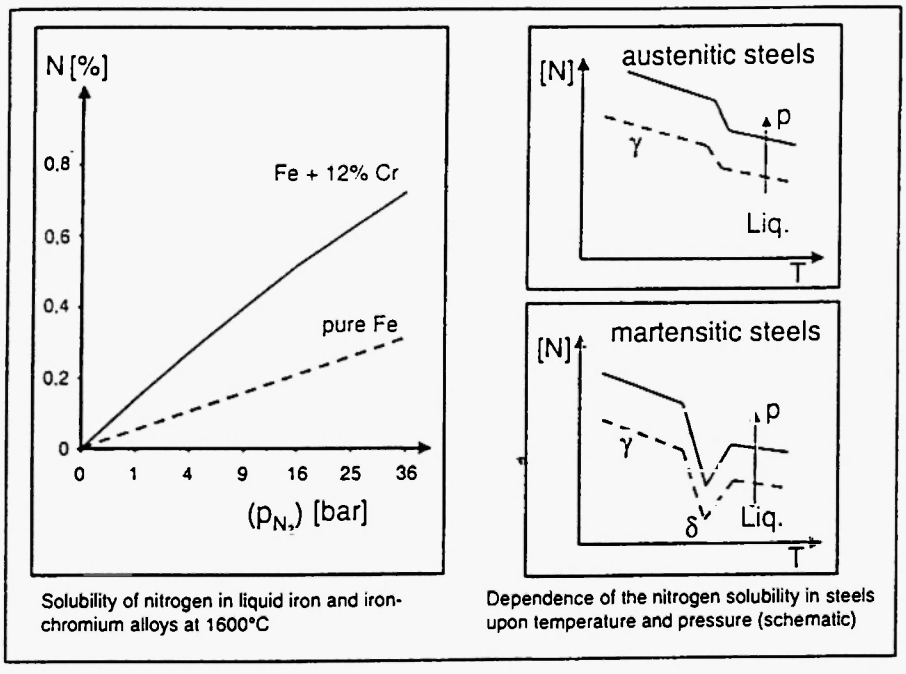

Solubility of nitrogen in liquid iron and iron-chromium alloys at 1600°C

Dependence of the nitrogen solubility in steels upon temperature and pressure (schematic)

Fig. 19: Schematic of the dependence of the nitrogen solubility in austenitic and martensitic steels upon temperature and pressure. Solubility increases upon solidification in austenitic steels, while it decreases markedly during solidification in the δ ferrite range for martensitic steels /45/

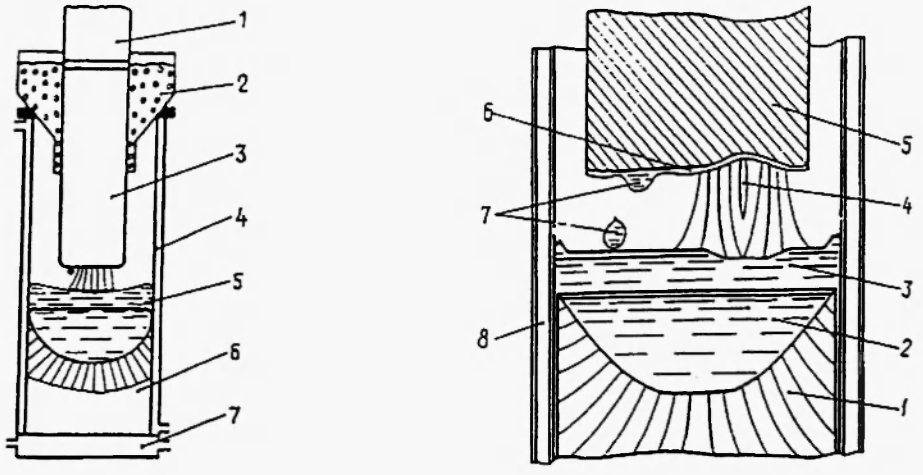

Fig. 20: a) Schematic of arc-slag remelting (ASR). 1) electrode feed mechanism; 2) flux gate; 3) electrode; 4) water cooled crystallizer; 5) liquid slag; 6) water cooled stool (after Medovar *et al.* /46/). b) ASR of a solid section electrode. 1) ingot; 2) metal bath; 3) slag bath; 4) electric arc; 5) consumable electrode; 6) liquid metal film; 7) droplets; 8) water cooled stool (after Medovar *et al.* /46/).

nitrogen absorption depends on the carbon content of the steel, probably relating to the formation and stability of the CN_2^{2-} in the slag. For high carbon tool steels, the rates are considerably higher than for the low carbon stainless steels. The operating pressure for most ASM processing is in the region of 1MPa, close to that for the equivalent ESR process.

Electron Beam Melting (EBM)

Electron beam melting, since it is necessarily carried out under high vacuum, has a high potential for nitrogen removal, but for the same reason is inappropriate for high nitrogen alloys. Generally, the operating vacuum is in the region of 0.1 – 0.5 Pa ; the melt has a higher surface temperature and a higher surface/volume ratio than the other processes considered. Importantly, since a water-cooled copper container keeps the melt away from contact with refractories, the surface oxygen content is likely to be reduced into the region of high nitrogen transfer rates through the clean surface /48/. Nakamura and Kuwabara /48/ investigated nitrogen removal during EBM of a high chromium steel, and were able to reduce nitrogen content to levels below 100 ppm, a value below that attainable by conventional melting techniques. McAllister and Mihalisin /49/ were able to attain reduction from 95 ppm to 20 ppm for a superalloy. The rate of nitrogen removal /48/ is calculated as

$$\Phi = k(a_N)^n = k(f_n[\%N])^n \qquad (24)$$

where k is the apparent rate constant, a_N and f_n are the activity and activity coefficient of nitrogen repectively, and the value of n depends on the rate controlling step (one for mass transfer across a boundary layer and two for chemical reaction control). It was predicted that lower levels of nitrogen should be attainable by decreasing the rate of melting, but with the concurrent problem of an unacceptable level of chromium evaporation.

It is also suggested /9/ that the electron beam process could be advantageous for removal of nitrogen through the removal of particulate TiN. While the temperature under the incident beam is high, in general the overall bath temperature can be kept low by suitable arrangement of the beam scanning system. Additionally, TiN particles floating on the bath surface and intercepted by the electron beam will decompose, providing an important addition to TiN removal by

physical means /9/. A technique of removing the surface oxides by utilising the surface flows created by the Maragoni forces is frequently used to remove the surface nitrides and also any surface oxides ("Electronic Dam") /50/. Once all the solid TiN has been removed, the low pressure regime of EBM will operate to remove nitrogen according to Sieverts' Law. This situation has been realised commercially /50/ in the re-cycling of superalloy scrap, particularly for the expensive single-crystal casting alloys, where extremely low (< 4 ppm) nitrogen contents are mandatory.

Plasma Arc Processing

Although most of the processes discussed thus far are concerned with nitrogen removal, nitrogen, as indicated above, can have many beneficial effects on several grades of steels /51/, and any method which offers the potential for the addition of nitrogen to steels is of practical interest, as discussed above for ESR and the arc-slag process. Another possibility is the process of nitrogen plasma melting, since plasma ionisation permits nitrogen contents far in excess of those predicted by N_2 – based thermodynamics to be achieved /52/. In general the final nitrogen content is described by the dynamic equilibrium between the rate of absorption directly under the plasma arc and the rate of desorption from the rest of the bath (which is not exposed to the ionisation equilibrium existing in the plasma itself, containing up to 10 wt % N^+ ions when the plasma gas is pure nitrogen). Thus high nitrogen contents are achieved only when there is a high contact area between metal and plasma arc, or when the liquid is quenched by atomisation or an equivalent process /52/.

Guangqian *et al.* /53/ conducted an investigation of nitrogen-bearing stainless steel production and found that the absorption is controlled primarily by the partial pressure of oxygen in the nitrogen plasma gas, alloying time and steel temperature, and that nitrogen contents of 0.2 – 0.3 wt% for 18-8 stainless steel were attained. Similar high nitrogen contents were reported by Lian and Chen /54/ who attained 3000 ppm nitrogen in Fe-20Cr-6Mn-5Ni-N stainless steel. Summarizing the results of Guangqian *et al.* /53/, the nitrogen content of stainless steel after plasma arc melting is given by;

$$\ln [N] = -16.71+10^{-0.2}\ln Q - 0.29\ln P_{N2} + 0.23\ln P_{O2} +0.22\ln D + 0.75\ln t + 1.37\ln T \quad (25)$$

where Q is the gas volume from bottom blowing, P_{N2} and P_{O2} are the partial pressures of nitrogen and oxygen in the plasma gas, D is the gun position, t is the alloying time, and T is the steel temperature. It is reported that the error in this relation is less than 10% /53/, in spite of the apparently-contradictory finding that the nitrogen content is enhanced by the presence of oxygen. This observation could possibly be explained by the fact that in the high-temperature, high p_N^+ regime of the plasma, the surface oxygen content of the alloy is not high enough to influence the nitrogen transfer rate, but in the bath region away from the plasma target zone, the oxygen content is high enough to prevent desorption of nitrogen gas towards the Sieverts' equilibrium, hence giving an overall nitrogen content which is positively influenced by oxygen concentration.

Another plasma arc process of interest is that of plasma arc remelting, which can be used for inclusion removal in nickel- base superalloys, as investigated by Brown *et al.* /55/. In this case, it is suggested that the nitrogen reduction occurs by a dissociation reaction into the low p_{N2} environment of the hydrogen/helium plasma;

$$2TiN\ (s) \rightarrow 2[Ti] + N_2\ (g) \quad (26)$$

which is enhanced by the localized heating beneath the plasma torch. Titanium is then retained in the melt and nitrogen is removed as an exhaust gas. Indeed, nitride levels were easily reduced to acceptable (< 37 ppm) levels in IN 718 when a hydrogen/helium plasma torch gas was used, and a marked reduction in inclusion content was observed. Unfortunately however, the superior nitrogen removal was overshadowed by oxide contamination during the melting process, a factor that is being investigated to increase the feasibility of plasma arc remelting as a viable production route for superalloys.

SUMMARY

The basic thermodynamics and kinetics surrounding the exchange of nitrogen in the special melting

processes are well understood and can be applied for the analysis of the individual processes. Extensive literature is available, providing information on both the physical parameters involved and on the nature of the reactions. It is to be noted that the nitrogen solubility in the three principal alloy-forming elements, Fe, Cr and Ni, is very different. Under atmospheric pressure nitrogen, nickel has an almost zero solubility for nitrogen, iron a significantly higher solubility and chromium a high solubility. These differences are clearly reflected in the results of processing the various alloys considered in this report.

Each process has advantages and disadvantages with respect to nitrogen control; VIM, VAR and EB involve low pressures enabling nitrogen removal according to Sieverts' Law, provided the conditions are correct, and VIM has the added advantage of induction stirring, inclusion attachment to the crucible walls and also filtering. In VAR inclusions can be removed by agglomeration and flotation, but since the process involves an isolated heating cycle, we must take into account the appropriate solution/re-precipitation mechanisms that would preclude inclusion removal or modification. ESR offers some nitrogen removal by solution in the slag, but, like VAR also contains a solution/precipitation scheme, in this case additionally modified by the concurrent change in the nature of the oxide inclusions. To obtain the full benefit of the ESR mechanisms, it is clearly necessary to operate the process with argon protection to prevent nitrogen pick-up from the atmosphere, or with an overpressure of nitrogen to retain high nitrogen contents in the appropriate alloy systems. Electron beam melting offers great potential for nitrogen removal, but at the cost of added process complexity. Plasma processing, either by using the plasma as an augmentation in an induction-heated system, or as a remelting process, offers the potential of high nitrogen addition through the ionisation process. The ASM process offers essentially the same advantages, at a much lower cost, through the same ionisation mechanism. Neither process has been shown to provide any additional advantage in removing oxide inclusions at the same time as nitrogen modification.

In all cases, low-nitrogen raw materials are a critical component of the cost equation concerning nitrogen behaviour during specialty processing. Since, in the presence of realistic levels of oxygen, the nitrogen removal rates from liquid alloys are extremely slow, in many cases it is more reasonable to use expensive raw materials than it is to absorb the additional cost of lengthy melt-processing. The basis for process selection and design involves all of the above considerations, but the basic process parameters for excellent nitrogen control are clear and available.

REFERENCES

1. Huang, X., Zhang, Y. and Hui, Z., *Metall. Mater. Trans. A,* **30A**, 1755 (1999).
2. Gaskell, D.R., *Introduction to the Thermodynamics of Materials, 3rd ed.*, Taylor and Francis, Washington D.C., 1995.
3. Pehlke, R.D. and Elliott, J.F., *Trans. Metall. Soc. AIME,* **218**, 1088 (1960).
4. Rao, Y.K. and Lee, H.G., *Ironmaking Steelmaking,* **12**, 209 (1985).
5. Humbert, J.C. and Elliott, J.F., *Trans. Metall. Soc. AIME,* **218**, 1076 (1960).
6. Wada, H. and Pehlke, R.D., *Metall. Trans. B,* **8B**, 443 (1977).
7. Shahapurkar, D.S. and W.M. Small, *Metall. Trans. B,* **18B**, 231 (1987).
8. Saito, T., *Proceedings of the 4th International Conference on Vacuum Metallurgy,* ed. Inouye, M., Tokyo, ISIJ, 1973.
9. Cockcroft, S.L., Degawa, T., Mitchell, A., Tripp, D.P., Schmaltz, A., *Superalloys 1992*, eds. Antolovitch, D *et al.*, TMS, 1992, p.577.
10. Mitchell, A., *Advanced Materials and Processing Techniques,* ed. Froes, F.H., ASM, Paris, 1987, p.233.
11. Liao, L. and Fruehan, R.J., *Trans. Iron Steel Soc. AIME,* **16**, 91 (1989).
12. Ozturk, R., Matway, R. and Fruehan, R.J., *Metall. Trans. B.*, **26B**, 563 (1995).
13. Mitchell, A., *Conference Proceedings; P/M in Aerospace, Defense and Demanding Applications,* ed. Froes, F.H., MPIF, New Jersey, 1993, p.333.
14. Turkdogan, E.T., *Trans. Iron Steel Soc. AIME,* **16**, 61 (1989).

15. Sano, N., Lu, W-K., Riboud, P., eds., *Advanced Physical Chemistry for Process Metallurgy,* Academic Press, London, 1997.
16. Battle, T.P. and Pehlke, R.D., *Ironmaking Steelmaking,* **13**, 176 (1986).
17. Pehlke, R.D. and Elliott, J.F., *Trans. Metall. Soc. AIME,* **227**, 844 (1963).
18. Fruehan, R.J. and Martonik, L.J., *Metall. Trans. B,* 11B, 1980, p.615.
19. Choh, T., Moritani, T., Inouye, M., *Proceedings of the 6th Vacuum Metallurgy Conference on Special Melting,* eds. Bhat K and Lherbier, L., American Vacuum Society, New York, 1979, p.225.
20. Byrne, M. and Belton, G.R., *Metall. Trans. B.,* **14B**, 441 (1983).
21. Kobyashi, A., Tsukihashi, F., and Sano, N., *ISIJ Int.,* **33**, 1131 (1983).
22. Glaws, P.C. and Fruehan, R.J., *Metall. Trans. B,* **16B**, 551 (1985).
23. Oriani *et al.*, eds, *Physical Chemistry in Metallurgy,* U.S. Steel Corporation, Pittsburgh, 1976.
24. Ono, H., Morita, K., and Sano, N., *Metall. Trans. B,* **26B**, 991 (1995).
25. Hajra, J.P. and Divakar, M. *Metall. Mater. Trans. B,* **30**, 429 (1999.
26. Machlin, E.S., *Trans. Metall. Soc. AIME,* **218**, 314 (1960).
27. Pettinicolas, L. Jardy, A. Ablitzer, D., *Proceedings of the 1997 International Symposium on Liquid Metal Processing,* eds. Mitchell, A. and Auburtin, P., American Vacuum Society, 1997, p.390.
28. Darmara, F.N., *J. Met.*, 19, 42 (1967).
29. Leinbach, R.C. and Hamjian, H.J., *J. Met.,* **18**, 219 (1966).
30. Mitchell, A., *Special Melting and Processing Technologies,* ed. Bhat K, Noyes Publications, New Jersey, 1988, p.147.
31. Simkovich, A., *Proceedings, Electric Furnace Conference,* TMS, 1965, p.170.
32. Aksoy, A.M., Thermodynamics and Kinetics in Vacuum Induction Melting, *Vacuum Metallurgy,* Reinhold Publishing Corp., New York, 1958, p.59.
33. Bieber, C.G., and Decker, R.F., *Trans. Metall. Soc. AIME,* **221**, 629 (1961).
34. Katayama, H. and Nakamura, Y.,*Proceedings of the 7th International Conference on Vacuum Metallurgy,* ed. Inouye, M., ISIJ, Tokyo, 1982, p.933.
35. Chen, F., Huang, X., Wang, Y., Zhang, Y. and Hu, Z., *Mater. Lett.,* **34**, (372 (1998).
36. Apelian, D. Mutharasam, R. Romanowski, C., *Report # AMMRC TR-80-16, Army Materials and Mechanics Research Center,* April, 1980.
37. Fu, J., Zhao, J.H., Wang, H., and Xu, G.Y., *Special Melting and Processing Technologies,* ed. Bhat, K., Noyes Publications, New Jersey, 1988, p.722.
38. Quested, P. Hayes, D.M., *Proceedings of Electron Beam Melting Conference,* ed. Bakish, R., Bakish Materials Corp, Englewood NJ, 1994, p.6.
39. Tommaney, J.W. and Ramachandran, S., *Proceedings of the Electric Furnace Conference,* TMS, 27, 1969, p.21.
40. Mancuso, S. Sczerzenie, F.E. Maurer, G., *Superalloys 1988*, ed. Duhl. D.N., TMS 1988, p.377.
41. Sutton, W.H., *Proceedings of the 7th International Conference on Vacuum Metallurgy,* ed. Inouye, M., Japan Iron & Steel Institute, Tokyo, 1982, p.904.
42. Martinez, E., Espejo, O.V. and Majarrez, F., *ISIJ. Int.,* **33**, 48 (1993).
43. Elissa, M.M, Mattar, T.M. and El-Fawakhry, K.A., *Proceedings of the 5th International Conference on Tooling,* eds. Jeglitsch, F. Ebner, R. Leitner, H., University of Leoban, Leoben, Austria, 1999, p.275.
44. Mitchell, A., Melting Processes and Solidification in Alloys 718-625, *Superalloys 718, 625 and Various Derivatives,* ed Loria, E. TMS, 1991, p.15.
45. Schnieder,R. Koch, F Wurzinger, P., *Proceedings 5th International Conference on Tooling,* eds. Jeglitsch, F. Ebner, and Leitner, H., University of Leoban, Leoban, Austria, 1999, p. 265.
46. Medovar, B. I. Saenko, V.Y. Grigorenko, G.M. Pomarin, Y.M. and Kumysh, V.I., *Arc-Slag Remelting of Steel and Alloys*, Cambridge International Science Publishing, England, 1995.
47. Paton, B.E. Medovar, B.I. Lebedev, V.K. and Saenko, V.Y., *Metallurg,.* **10**, 17 (1974).
48. Nakamura, Y. and Kuwabara, M., *Trans. Iron Steel Inst. Jpn.,* **16**, 122 (1976).

49. McAllister, R.C. and Mihalisin, J.R., "Electron Beam Refining of Vacuum Induction Remelt Stock", Internal Report, Howmet Turbine Components Corporation/Alloy Division, Dover NJ.
50. Haruna, Y. Mitchell, A. Schmalz, *Proceedings, International Conference on Electron Beam Melting*, ed. R Bakish, Bakish Corp, Englewood NJ, 1994, p. 156.
51. Reed, R.P., *JOM*, **41**, 16 (1989).
52. Gammal, T.E., Hinds, G. and Mokrov, I., *Proceedings of the 6th International Conference on Vacuum Metallurgy*, eds. Bhat, K and Schlatter, R, American Vacuum Society, 1979, p.465.
53. Guandquian, F. *et al.*, *Proceedings of the 10th International Conference on Vacuum Metallurgy*, eds. Fu, J. Zhang, R. Xie, Y. and Bloore, E. Metallurgical Industry Press, Beijing, 1990, p.196.
54. Shuang-shii, L. and Chen, T.S., *International Symposium on Liquid Metal Processing and Casting*, eds. Mitchell, A. and Fernihough, J., American Vacuum Society, 1994, p.54.
55. Brown, D.N., Young, J.M., Jacobs, M.H. and Patel, S.J., *Proceedings of the 1997 International Symposium on Liquid Metal Processing*, eds. Mitchell, A. and Auburtin, P., American Vacuum Society, 1997, p.403.
56. Deo, B. and Boom, R., *Fundamentals of Steelmaking Metallurgy*, Prentice Hall International, NewYork, 1993.